PHYSICAL REVIEW C **86**, 015805 (2012)

$^{12}C(\alpha, \gamma)^{16}O$ studied with the Karlsruhe 4π BaF_2 detector

R. Plag* and R. Reifarth
Goethe-Universität Frankfurt am Main, Max-von-Laue-Strasse 1, 60438 Frankfurt am Main, Germany

M. Heil
GSI Darmstadt, Planckstrasse 1, 64291 Darmstadt, Germany

F. Käppeler, G. Rupp, F. Voss, and K. Wisshak
Karlsruhe Institute of Technology, Campus North, Institute of Nuclear Physics, P.O. Box 3640, 76021 Karlsruhe, Germany
(Received 5 March 2012; published 5 July 2012)

The $^{12}C(\alpha, \gamma)^{16}O$ reaction is one of the most important in nuclear astrophysics since it determines the ratio of ^{12}C to ^{16}O during stellar helium burning. Experimental data, however, are still subject to large uncertainties due to the almost vanishing cross section at stellar energies. So far, most measurements have been performed with germanium detectors. To compensate for their low efficiency, the highest beam currents had to be used, resulting in target degradation and beam-induced backgrounds. Instead, the present measurement was performed with high-efficiency detectors and low beam currents, using the Karlsruhe 4π BaF_2 detector and the pulsed 3.7-MV Van de Graaff accelerator at Karlsruhe Institute of Technology. The $^{12}C(\alpha, \gamma)^{16}O$ cross sections have been measured at center-of-mass energies E between 1002 and 1510 keV, and the $E1$ and $E2$ components were derived with an accuracy comparable to the previous best data obtained with HPGe detectors.

DOI: 10.1103/PhysRevC.86.015805 PACS number(s): 25.40.Lw, 25.55.−e, 26.20.Fj, 27.20.+n

I. INTRODUCTION

The $^{12}C(\alpha, \gamma)^{16}O$ reaction has a long historic record in nuclear astrophysics. Already early on Burbidge *et al.* [1] noted that "one of the most pressing current problems in element synthesis is the need for experimental measurements on $^{12}C(\alpha, \gamma)$." In spite of numerous attempts to solve this problem, the statement that the $^{12}C(\alpha, \gamma)^{16}O$ rate represents "the single greatest experimental uncertainty in explosive nucleosynthesis," made by Arnett [2] more than four decades ago, still holds today.

The importance of the $^{12}C(\alpha, \gamma)^{16}O$ reaction results from the fact that it determines the uncertainty of the carbon to oxygen ratio at the end of He burning, the production of carbon being well characterized by the triple α reaction [3]. This uncertainty propagates into the abundance yields up to Fe that are produced during the later stages in the evolution of massive stars, i.e. during C, Ne, O, and Si burning [4,5], and has a significant effect on the final supernova [6] as well as on the fate of the remnant neutron star or black hole [7]. The $^{12}C(\alpha, \gamma)^{16}O$ rate is also important for the evolution of low mass stars, where it affects the transition to carbon stars [8] and the formation of SiC grains [9].

The intriguing aspects of the $^{12}C(\alpha, \gamma)^{16}O$ reaction have triggered intense experimental efforts over the last 50 years. The many experimental attempts have been summarized and condensed into the recommended values reported by Caughlin and Fowler [10] and more recently by the NACRE Collaboration [3]. Since this last compilation, new data became available from measurements with α beams [11–13] as well as by employing inverse kinematics [14] and indirect methods [15–18] and from experiments with recoil mass separators [19–21].

Over the course of these studies, the experimental approaches have been continuously refined and extended. In 1970 and 1974, Jaszczak and co-workers [22,23] and Dyer and Barnes [24] started out with fairly complete experiments, using a pulsed α beam for background suppression, isotopically pure ^{12}C targets, and large NaI(Tl) crystals for measuring the cross section down to a c.m. energy of 1.41 MeV. In addition, Dyer and Barnes measured γ-ray angular distributions at higher energies. The sensitivity of these experiments was later improved by replacing the NaI(Tl) crystals by large Ge detector arrays of increasing complexity. Since the gain by the higher resolution in γ-ray energy was somewhat compensated by the lower γ-ray efficiency, very intense α beams had to be used [11–13,25,26]. In these experiments the α energy has been pushed to a lower limit of $E_{\text{c.m.}} = 0.891$ MeV, and angular distributions were obtained down to $E_{\text{c.m.}} = 1.3$ MeV.

Complementary to investigations with α beams, a number of investigations were carried out in inverse kinematics using ^{12}C beams on a windowless He gas target. This approach [14,27,28] offers the advantage that there are no problems with target stability. In combination with a mass separator [29] this technique has also been used to obtain essentially background-free reaction yields by γ-recoil coincidences [29]. Also, γ-ray angular distributions have been studied for separating the $E1$ and $E2$ contributions in the capture transitions [30].

More recently, recoil mass separators have been developed with sufficient resolution to count the ^{16}O nuclei produced in $^4He(^{12}C, \gamma)^{16}O$ reactions essentially free from interference with the primary ^{12}C beam [31,32]. This technique allows one to determine the total reaction cross section, independent of the individual contributions coming from the involved resonances and from the direct capture component. The first results

*r.plag@gsi.de

from such measurements were reported for $E_{c.m.}$ energies down to 1.9 MeV [19,21,33]. Further extension of these measurements to lower energies is presently hampered by residual backgrounds.

In addition to the direct investigations sketched above, important additional data have been obtained by indirect methods. The competing channel for elastic scattering was remeasured over a large energy range with significantly improved angular resolution [34], yielding significant information on the involved nuclear levels and their contribution to the overall reaction rate. The β-delayed α decay of ^{16}N [15,16] and sub-Coulomb α transfer [17,18] are other examples in this respect.

Summarizing the situation one finds that the important low-energy data for the $^{12}C(\alpha,\gamma)^{16}O$ cross section are not only affected by comparably large uncertainties but exhibit also sizable discrepancies. Since the low-energy data were all obtained with intense α beams and solid state targets, a new approach has been developed in this work, by replacing the HPGe detectors with a 4π array of BaF_2 detectors with nearly 100% detection efficiency for γ rays. In this measurement, systematic uncertainties were well under control because backgrounds were efficiently suppressed by using a fast pulsed α beam and because target deterioration was strongly reduced due to the low average beam currents on target. Moreover, angular distribution measurements could be performed to much lower energies by taking advantage of the 42-fold geometry of the 4π array. With this type of detector, the contribution of cascade transitions to the total (α,γ) cross section could be determined as well.

The experimental details concerning the detector and the data acquisition system are described in Secs. II and III, followed by a discussion of samples and experimental backgrounds (Sec. IV) and the actual measurements and the procedures used in data analysis (Secs. V and VI). The deduced cross sections are presented in Sec. VII.

II. THE KARLSRUHE 4π BaF_2 DETECTOR

The Karlsruhe 4π BaF_2 detector [35] was designed for high γ-ray efficiency at a comparably low neutron sensitivity. The detector (Fig. 1) is divided into 42 hexagonal and pentagonal segments and covers 97% of 4π solid angle. Each segment, except one for the beam entrance, holds an independent detector module consisting of a BaF_2 scintillator crystal. The crystals are shaped as truncated pyramids, which form exactly a spherical shell of 15 cm in thickness with a 10-cm inner radius. Because of the high density of BaF_2 and the comparatively high atomic number of Ba, a total detection efficiency of more than 90% is reached with this detector up to γ-ray energies of 10 MeV.

The segmentation of the detector and the fact that all crystals cover the same solid angle with respect to the center allows measurements of the reaction yield simultaneously at 12 different angles with respect to the beam axis. This feature is necessary since the γ angular distributions are needed for extracting the $E1$ and $E2$ components of the $^{12}C(\alpha,\gamma)^{16}O$ cross section from the measured yields, information that is crucial for a reliable extrapolation to astrophysical energies.

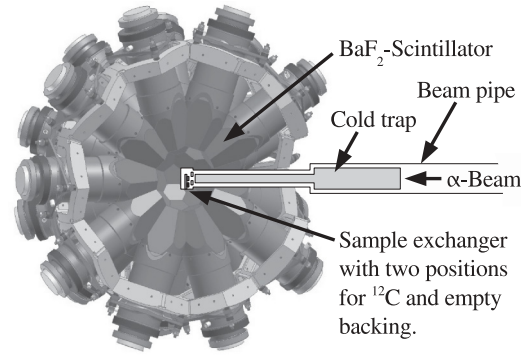

FIG. 1. The Karlsruhe 4π BaF_2 detector, consisting of 42 independent modules forming a spherical shell of BaF_2 that is 15 cm thick and has an inner radius of 10 cm.

In spite of the 60 l total scintillator volume, an overall time resolution better than 1 ns can be routinely obtained with the 4π detector thanks to a fast component in the scintillation light of BaF_2 with a time constant of 0.6 ns. This makes the detector well suited for time-of-flight (TOF) applications, a feature that was also used in the present experiment.

Prior to the measurements, the energy response of the detector modules was calibrated at 0.62, 1.17, 1.33, and 6.13 MeV with standard Cs, Co, and Pu/C sources. In order to maintain the energy resolution of about 6% for sum energies around 6 MeV, possible small gain drifts in the individual modules due to temperature effects had to be constantly measured and compensated by modifying the high-voltage settings of the photomultipliers. This check was performed regularly by measuring the intrinsic α activity from the decay of ^{214}Po, a daughter of ^{226}Rn, a chemical homolog to Ba, which occurs as a natural impurity in BaF_2. Signals induced by α particles are significantly different in shape compared to those produced by γ rays. Hence, an almost background-free α spectrum can be obtained by means of a fast wave form digitizer, i.e., a 500-MHz flash amplitude digital converter (FADC), and subsequent wave form analysis on a personal computer (PC). Depending on the different α rates of the individual detector modules, acquisition of a sufficiently accurate α spectrum takes between one and five minutes. Since the modules are tested sequentially, each detector is checked and—if necessary—gain adjusted every two hours, an interval much shorter than that over which the observed gain drifts.

III. THE DATA ACQUISITION SYSTEM

The data acquisition system was based on the FERA [Fast Encoding and Readout ADC (analog-to-digital converter)] system of LeCroy connected to a PC via a CAMAC (Computer Aided Measurement And Control) interface. The TOF and energy signals of each individual detector module were converted by Model 4300B FERA ADCs with a resolution of 11 bits. The TOF signals were provided by Model 4303 TFCs (time-to-FERA converters). The converted data were

buffered in one of two 4302 memories, which were read out alternately by a PC practically free of dead time. The PC ran a custom-built data acquisition program for writing the data event by event (list mode) to hard disk, optionally after applying a data reduction procedure. It provided also a graphical online data analysis, which was sufficient to verify that the whole system worked properly.

Since the data rate of this experiment was comparatively low, any data reduction mechanisms had been disabled. In this way, the full information on the backgrounds in both channels, energy and TOF, was recorded as well. This option turned out to be very useful for a comprehensive and detailed data analysis.

IV. SAMPLES AND RELATED BACKGROUNDS

One of the main difficulties in the direct measurement of the $^{12}C(\alpha,\gamma)^{16}O$ reaction rate is background from concomitant $^{13}C(\alpha,n)^{16}O$ reactions due to ^{13}C impurities. Since the (α,n) rate of ^{13}C is about five orders of magnitude higher than the (α,γ) rate of ^{12}C, depletion of ^{13}C in the sample material is a crucial issue.

The samples for this experiment have been produced in the isotope separator SIDONIE at CSNSM, Orsay, France, in the same way as had been worked out for previous experiments [36]. The ^{12}C was deposited with an energy of only 200 eV on a gold-coated copper backing or directly onto a very pure (99.9999%) copper backing until very stable layers between 30 and 120 $\mu g/cm^2$ had been obtained. The 120 $\mu g/cm^2$ thick samples could preferentially be used for improving the measured count rates at low energies, because the energy loss in the sample required only a comparably small correction.

The samples produced at SIDONIE were strongly depleted in ^{13}C and showed $^{12}C/^{13}C$ ratios larger than 9×10^5, corresponding to a depletion in ^{13}C (1.1% in natural carbon) by a factor 10^4. The samples turned out to be extremely stable under α bombardment. Even after irradiation with an integrated α beam of 1.6 C no significant degradation could be observed.

The thickness of each sample was determined before and after the actual runs by scanning the narrow 2^+ resonance in the $^{12}C(\alpha,\gamma)^{16}O$ cross section at $E_{c.m.}=2.68$ MeV. The differences before and after the individual runs were always well below the 4% to 6% uncertainty of the thickness measurement itself. A representative thickness profile is shown in Fig. 2.

Carbon buildup on the sample turned out to be a persisting problem, which could never be completely prevented in spite of using an 84-cm-long liquid nitrogen cold trap directly in front of the ^{12}C target. While buildup left the amount of ^{12}C practically unchanged, the amount of ^{13}C increased significantly.

However, even for fresh, fully depleted targets, the $^{13}C(\alpha,n)^{16}O$ rate dominates that of the $^{12}C(\alpha,\gamma)^{16}O$ reaction. The resulting neutron-induced background could not be completely suppressed because of the large volume of the BaF_2 scintillator, although the intrinsic neutron sensitivity is much smaller compared to HPGe detectors. The necessary further suppression of the ubiquitous ^{13}C background was achieved

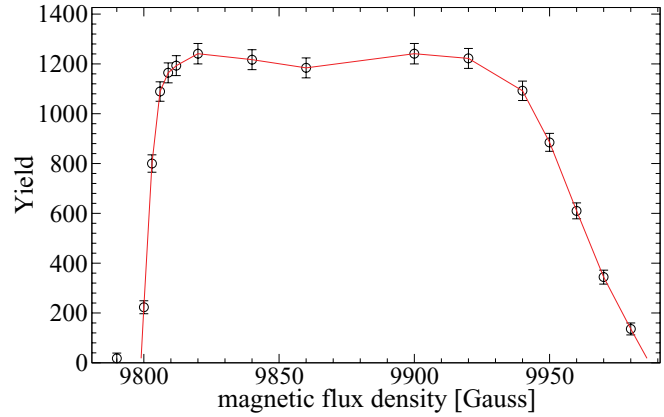

FIG. 2. (Color online) Thickness profile of the ^{12}C layer obtained by scanning the narrow 2^+ resonance at 2.68 MeV. The scan was performed with the same detector setup as the cross-section measurement.

by means of the fast pulsing system of the Karlsruhe Van de Graaff accelerator. In this case, the prompt γ rays from (α,γ) reactions appear in the TOF peak marking the impact of the α pulse on the target, whereas by far most of the neutron background appears with a significant delay. This is illustrated in Fig. 3, which shows the delayed response of the 4π BaF_2 array to neutrons. An additional background component prior to the prompt signal from the ^{12}C sample is caused by α particles outside the main beam (e.g., due to the beam halo). This component, which is timewise fully correlated with the main beam, is hitting the cold trap a few centimeters before the target and is, therefore, not contributing to the prompt signals at time zero.

For better characterization of the remaining background, an additional set of data was taken with an empty backing. Both the ^{12}C targets and the empty backing have been mounted on a small, integrated sample changer. The sketch of Fig. 4 shows the compact target design that had to fit into the limited space inside the BaF_2 detector indicated by the

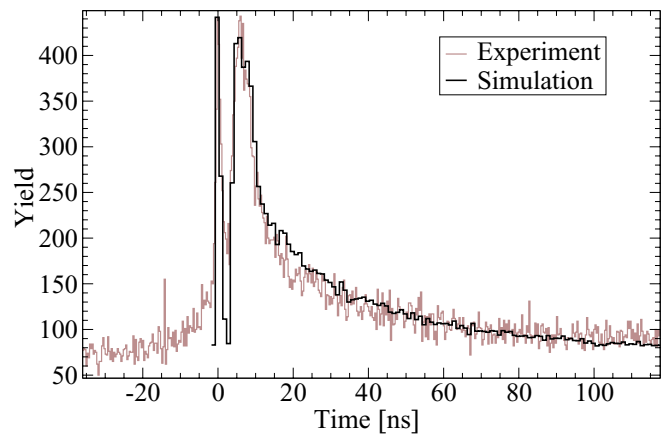

FIG. 3. (Color online) Measured TOF spectrum demonstrating the efficient discrimination between prompt γ rays from radiative capture events and the delayed detector response to neutrons. In the GEANT simulation the 2-ns pulse width of the α beam was not considered (see text).

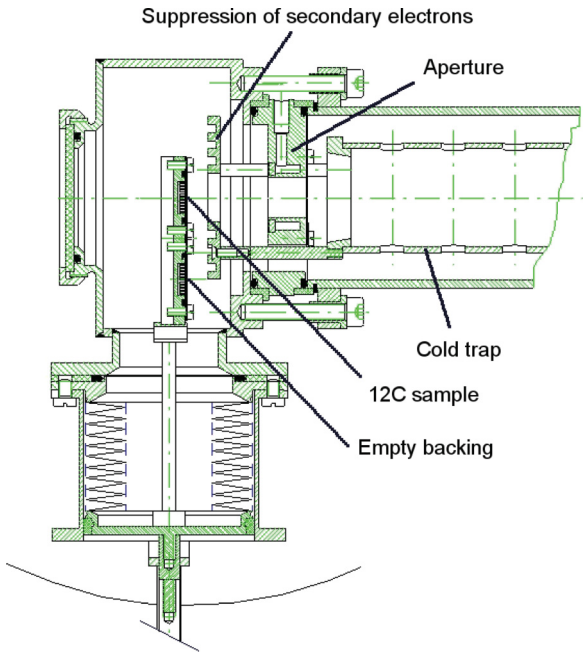

FIG. 4. (Color online) A sample exchanger with two samples (^{12}C and empty backing) installed in the center of the detector. The aperture as well as the disk for the suppression of secondary electrons were coated with very pure gold to avoid background if hit by the α beam.

curvature at the bottom. The ^{12}C target and the empty backing were automatically interchanged after a preselected charge was accumulated, typically every 20 min. In this way, slow fluctuations in the α beam were averaged over both samples and do not contribute to systematic uncertainties.

The background from cosmic rays was reduced by an active shielding consisting of a 1.9×1.9 m^2 plastic scintillator, which was mounted on top of the 4π detector. Further shielding was available but was not used since the overall background was dominated by the contributions from the α beam.

V. MEASUREMENTS

During the measurements the α beam was pulsed with a repetition rate of 1 MHz, with a pulse width of less than 2 ns and average beam currents of up to 6 μA. As shown in Fig. 4, a collimator with an aperture 8 mm in diameter defined the beam spot on the ^{12}C targets, which were prepared with diameters of about 15 mm.

The target chamber was insulated against the collimator and the beam line and worked as a Faraday cup for measuring the integrated charge. Secondary electrons were suppressed with a bias voltage of -200 V applied to the insulated cold trap, which ended in a disk in front of the target. During the runs the vacuum in the target chamber was 1.5×10^{-7} mbar.

The dead time of the setup was measured with a pulser that was connected to a free channel of the data acquisition system. The experiment was computer controlled with respect to the operation of the detector system as well as to the performance

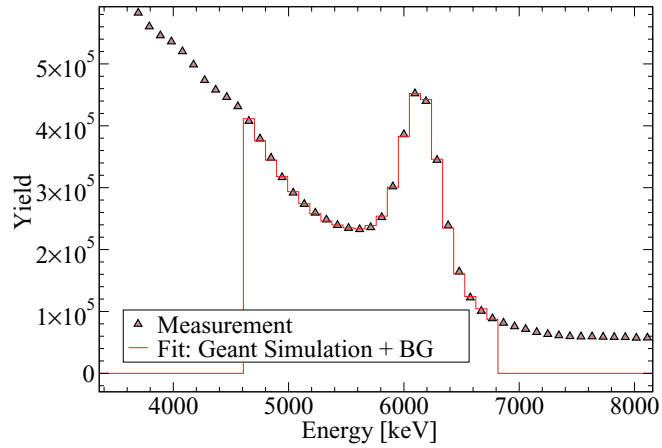

FIG. 5. (Color online) The γ-ray spectrum measured with a ^{238}Pu/^{13}C source (triangles) compared to a GEANT simulation, where the background was fitted by a third-order polynomial. Apart from the determination of the detector efficiency, this test was important for verifying the quality of the GEANT simulations used in data analysis.

of the accelerator. In this respect, the continuous control of pulse width and beam current was particularly important.

The sample, empty backing, and collimator were replaced once per week in order to keep the background from carbon buildup low.

The energy calibration of the α beam was obtained along with the measurement of the target profile. The beam energy corresponds to the leading edge of the profile (see Fig. 2), which can in principle be defined with an uncertainty of $\pm 0.02\%$. However, repeated scans of this resonance showed that the actual beam energy can be reliably reproduced with an uncertainty of only $\pm 0.1\%$.

The absolute γ-ray efficiency of the BaF_2 array depends slightly on the electronic threshold and is normally around 90%. The weak intensities obtained in the present experiment require a detailed simulation of the efficiency, which is described in the following section. The quality of the simulation was verified by means of the 6.13-MeV γ line from a calibrated ^{238}Pu/^{13}C source. Since this source is also emitting neutrons, it provided also a realistic background situation.

The γ-ray spectrum measured with this source is plotted in Fig. 5 (open triangles) and shows the 6.13-MeV line on top of a continuous background. Independently, this spectrum was simulated using GEANT3 [37] on the basis of an accurate computer model of the experimental setup, which considered all details of the 4π BaF_2 array including the experimentally measured energy resolution of the individual detector modules. In total 10^5 γ-ray histories were simulated, starting in arbitrary directions from the source in the center of the array. The simulated spectrum was then fitted together with a polynomial of third order for the background to match the measured distribution (Fig. 5).

In this fit the number of events is used as a free parameter that can be directly compared with the well-known number of γ rays emitted by the calibration source for defining the efficiency. Although only a 0.7% difference was found between simulation and experiment the corresponding uncertainty was estimated to be 5%. This value is motivated by the

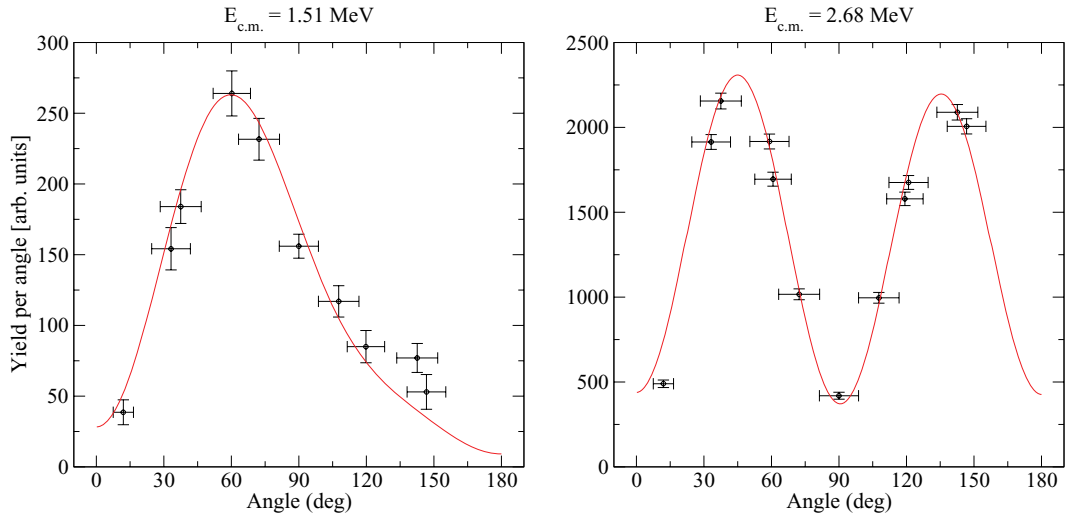

FIG. 6. (Color online) Angular distributions obtained at effective center-of-mass energies of 1.51 and 2.68 MeV. The vertical error bars represent statistical uncertainties only, the horizontal error bars indicate the angular range (1σ) of the corresponding detector array.

corrections required in the angular distributions, which showed an uncertainty of 10% at various angles (see below).

In the present experiment, the (α, γ) cross section has been measured at effective center-of-mass energies of 1002, 1306, 1416, and 1510 keV. In addition to the total cross section, the measurement provided also angular distributions of one-step transitions (Fig. 6) for the separation of the $E1$ and $E2$ contributions as well as the cross section of cascade transitions.

The accumulated charge for these measurements was between 0.75 and 2 C, corresponding to measuring times of 42 to 116 h per energy point.

VI. DATA ANALYSIS

A. The total (α, γ) cross section

A ^{12}C event is characterized by the related TOF and sum energy information, where the sum energy is given by the Q value plus the α energy $E_{\rm kin}$. Because of the short pulse width of the α beam, true capture events fall in a narrow line in the TOF spectrum, well separated from the neutron-induced background. The γ line in the energy spectrum, however, is less pronounced because of the 6% energy resolution of the BaF_2 array. In addition, the line exhibits a low-energy tail because γ rays after Compton scattering or pair production may escape detection because the detector is limited in solid angle (97% of 4π) and in absolute efficiency ($\approx$90%).

Therefore, an appropriate window was first applied to the TOF spectrum and the energy spectrum of these preselected events were fitted with the simulated ^{12}C spectrum and the background measured with the blank target. The measured background was slightly rescaled since it was 5% to 10% smaller than the background in the ^{12}C spectrum, presumably because the rate for carbon buildup was different for the two target surfaces. In this way, the correction for the efficiency of the detector was properly considered.

The quality of these fits is illustrated in Fig. 7 for an example of the run at 1430 keV α energy.

Since the low-energy part of the spectrum is dominated by background, the analyzed region starts at approximately 6 MeV and extends to 0.5 MeV above the peak. The total efficiency is reduced by 25% to 65% depending on the choice of the lower threshold. However, this loss in efficiency can be corrected by means of the GEANT3 simulations.

The results for the total cross section are included in Table I. Apart from the lowest energy point, the overall uncertainties are dominated by systematic effects. This is detailed by the compilation of uncertainties in Table IV. The systematic uncertainties are between 8% and 10% and are mostly determined by the TOF cut for optimizing the signal-to-background ratio. The uncertainty due to sample thickness refers to the determination of the areal density of the thin and thick ^{12}C layers. The quoted statistical uncertainties include a 4% contribution due the scaling of the background spectra measured with the blank backings.

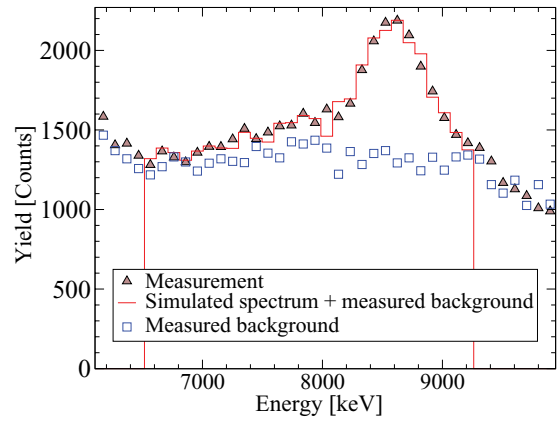

FIG. 7. (Color online) The γ-ray spectrum of ^{12}C(α, γ)^{16}O reactions at 1430 keV (triangles) and the corresponding GEANT simulation. The measured background was scaled to match the ^{12}C spectrum at energies above the peak. It is shown to illustrate the signal-to-background ratio.

TABLE I. Measured total $^{12}C(\alpha, \gamma)^{16}O$ cross sections.

$E_{c.m.}$ (keV)	Number of events	Time (h)	Charge (C)	σ_{tot} (10^{-11} b)
1002	2195	42	0.75	10 ± 4
1308	9548	116	2.055	36 ± 4
1416	4885	55	0.985	58 ± 6
1510	11921	65	1.16	83 ± 7

B. Angular distributions

Angular distributions are crucial for the separation of the important $E1$ and $E2$ components of the ^{12}C cross section. The 42-fold segmentation of the 4π BaF_2 array implies 13 different angles with respect to the incoming beam. In practice, angular distributions can be obtained only for 10 different angles because the position at 180° was blocked by the beam line, and two pairs of modules were too close to be resolved ($58° + 60°$ and $120° + 121°$).

To determine the multiplicity of an event, hits in neighboring modules were combined into clusters. In this way, cross-talk between the detectors could very well be compensated, especially since the original number of γ rays is small compared to the number of modules. In the following, "multiplicity" means therefore "number of clusters," which is a good approximation to the original number of γ rays.

Events with multiplicity 1 were selected to determine the raw angular distributions, which had to be corrected for differences in solid angles, for the cross-talking between neighboring detectors that affects angular distributions and multiplicities, and for scattering in the sample changer. Events with multiplicity 2 or higher could only be used for determining the total (α, γ) cross section, since the corresponding hit patterns were too complex to be disentangled reliably.

All corrections have been obtained by means of detailed GEANT3 simulations, which have been shown to reproduce the measured data very well [38]. The simulations were particularly useful for quantifying the correction for cross-talking, because this effect is responsible for events with multiplicity 1 being most likely distributed over a cluster of neighboring modules (for a detailed discussion see Ref. [39]). The simulations of the current setup were verified with calibration sources to confirm the simulated efficiency and the distortion of angular distributions by γ scattering.

The corrected angular distributions are given in Table II. These spectra were fitted by the expression

$$W(\theta_\gamma) = 1 - Q_2 P_2(\theta_\gamma) + (\sigma_{E2}/\sigma_{E1})\left[1 + \tfrac{5}{7} Q_2 P_2(\theta_\gamma) - \tfrac{12}{7} Q_4 P_4(\theta_\gamma)\right] + \tfrac{6}{5}(5\sigma_{E2}/\sigma_{E1})^{1/2} \cos\phi [Q_1 P_1(\theta_\gamma) - Q_3 P_3(\theta_\gamma)] \quad (1)$$

for deriving the ratio σ_{E2}/σ_{E1} and the phase shift ϕ. The terms $P_k(\theta_\gamma)$ are Legendre polynomials. The γ-attenuation factors

$$\begin{aligned} Q_1 &= 0.948, \\ Q_2 &= 0.927, \\ Q_3 &= 0.862, \\ Q_4 &= 0.775, \end{aligned} \quad (2)$$

which correspond to modifications of the solid angle per detector module because of the sample geometry and absorption losses in the sample changer, were also obtained by GEANT simulations of the 4π BaF_2 array.

The cross section ratio σ_{E1}/σ_{E2} and the partial cross section for decays with emission of single γ quanta can be used for calculating the partial cross sections σ_{E1} and σ_{E2}, which are listed in Table III in terms of the corresponding S factors. The phase shifts obtained in these fits are less relevant, because these data can be more precisely derived from R-matrix fits of the elastic scattering data [34].

TABLE II. Angular distributions.

Angle[a] (deg)	Number of modules	α energy (keV)			
		1002	1308	1416	1510
12.0	1	-1.5 ± 1.5	12 ± 5.6	4.4 ± 3.3	39 ± 1.5
33.2	2	12 ± 2.1	72 ± 7.7	15 ± 5.1	154 ± 2.1
37.5	4	16 ± 1.9	91 ± 6.1	12 ± 4.6	184 ± 1.5
59.1	2	26 ± 3.8	142 ± 11	32 ± 8.1	255 ± 2.9
60.7	4	18 ± 1.8	122 ± 7.3	31 ± 5.4	269 ± 1.7
72.3	4	15 ± 2.5	114 ± 7.7	34 ± 5.7	232 ± 1.7
90.0	8	13 ± 1.2	75 ± 4.2	21 ± 3.2	156 ± 0.8
107.7	4	11 ± 1.5	55 ± 5.1	13 ± 4.0	117 ± 1.3
119.3	4	12 ± 1.5	53 ± 5.4	8.0 ± 3.8	91 ± 1.2
120.9	2	12 ± 2.5	47 ± 7.5	6.7 ± 5.0	77 ± 1.7
142.6	4	5.7 ± 1.2	35 ± 5.7	7.8 ± 3.5	77 ± 1.1
146.7	2	3.6 ± 1.8	47 ± 8.6	6.8 ± 4.6	53 ± 1.6

[a]Effective angle with respect to incoming α beam.

TABLE III. Summary of results for S factors,[a] the $E1/E2$ ratio, and phase shift ϕ.

$E_{c.m.}$ (keV)	S_{tot} (keV b)	S_{casc} (keV b)	S_{E1} (keV b)	S_{E2} (keV b)	σ_{E2}/σ_{E1}	ϕ (deg)
1002	55 ± 20	16 ± 8.5	29 ± 15	10 ± 7.7	0.35 ± 0.3	67 ± 13
1308	30 ± 3.1	10 ± 3.1	14 ± 3.7	6.2 ± 2.4	0.44 ± 0.2	62 ± 8
1416	26 ± 2.6	6.5 ± 1.5	14 ± 3.3	5.7 ± 2.8	0.41 ± 0.3	55 ± 8
1510	23 ± 2.0	7.0 ± 1.5	12 ± 2.2	4.7 ± 1.5	0.40 ± 0.2	58 ± 6

[a]Listed are factors for the total (α,γ) cross section, the partial cross section for decays with two γ rays, and for the $E1$ and $E2$ components.

Compared to the situation of the total (α,γ) cross section, the uncertainties of the partial cross sections σ_{E1} and σ_{E2} are strongly influenced by the σ_{E1}/σ_{E2} ratio, which is very sensitive to the shape of the angular distributions. Already small deviations from the theoretical shape are giving rise to rather large uncertainties of the partial cross sections, as shown in the compilation of Table V. These uncertainties were evaluated by modifying the cross section ratio in the fits of the angular distributions until the χ^2 value differed by one unit. The statistical uncertainties in this part of the analysis include the uncertainties related to the determination of the event multiplicity, which have been estimated in a rather conservative way.

C. Cascade transitions

The ^{16}O product nucleus decays with a probability of 25% by two-step cascades, preferentially via the 2^+ and 1^- states at 6.9 and 7.1 MeV. In previous experiments, the detection of these events was hampered because the lines from the low-energy part of the cascades were situated in a region of high background. Therefore cascades could be considered only above $E_{c.m.} = 1.4$ MeV [25] and 2.0 MeV [11], whereas other recent experiments [26,36] did not include cross sections for cascades.

In this work, cascade transitions could be detected with a novel approach. Since the 4π BaF_2 array was operated as a segmented γ-ray calorimeter, cascades were identified by combining the well-defined sum energy with the event multiplicity. In this way the two lines associated with cascades could be separated. However, the energy resolution of the BaF_2 array was not sufficient to distinguish cascades via the 6.9-MeV state from those via the 7.1-MeV level. Therefore, only the sum of the cross sections for two-step cascades could be obtained. The corresponding S factors are given in Table III.

TABLE IV. Uncertainties of total (α,γ) cross section at measured energies (in percent).

Source of uncertainty	Uncertainty (%)			
	1002 keV	1308 keV	1416 keV	1510 keV
Sample thickness	4	5	6	5
Accumulated charge	3	3	3	3
γ efficiency	5	5	5	5
Cut in time of flight	20	5	5	1
Counting statistics	30	5	4	4

VII. RESULTS AND DISCUSSION

Since the 4π array was only available during a limited period of 16 weeks, the present measurement had to be restricted to four energies between 1000 and 1500 keV. The runs at higher energies were most useful for the assessment of the various systematic uncertainties whereas the lowest data point at 1002 keV was important to characterize the sensitivity of the present approach and the potential for extending the accessible range to even lower α energies.

Because of the very different technique applied in this work, the systematic uncertainties are completely independent from those in previous measurements. Moreover, the statistical uncertainties do not contribute significantly to the overall uncertainty (apart from the lowest data point at 1002 keV). Therefore, the first aspect is particularly important for resolving the discrepancies among previous data sets.

Unfortunately, this comparison is hampered by the fact that no experimental cross sections are given in most publications. Therefore, the comparison has to be based on the reported S_{E1} and S_{E2} factors, which carry also the additional uncertainties from the decomposition. As shown in Tables IV and V these uncertainties are already significantly larger than those of the total cross sections.

In terms of the S factors, the present results are in good agreement with the data given in Refs. [11,36]. This is illustrated in Fig. 8, where other data were excluded for better readability. It is interesting to note that the data set of Ref. [11] exhibits strongly fluctuating uncertainties, presumably because of limitations in counting statistics. In particular, the lowest data point is so strongly dominated by the uncertainty that the physical information practically vanishes.

A brief summary of the comparison with other previous data shows that the results of Roters *et al.* [14] for the ratio σ_{E2}/σ_{E1} agree with this work above 1.3 MeV, but they are strongly discrepant at lower energies. Within uncertainties the S_{E1} values of Ouellet *et al.* [26] are in agreement at 1.4 MeV, but the corresponding S_{E2} data are higher by a factor of 2. The results of Kremer *et al.* [29] for S_{E1} at 1.3 and 1.5 MeV show good agreement, whereas the S_{E1} values of Redder *et al.* [25] between 1.3 and 1.5 MeV are systematically higher by more than 60% on average. Similarly, the contribution of cascade transitions reported by these authors at 1.4 MeV are higher by a factor of 3 compared to the values given in Table III. The S_{E1} data obtained in the pioneering work of Dyer and Barnes [24] are in agreement at 1.4 MeV, but they suffer from large uncertainties.

TABLE V. Uncertainties related to analysis of angular distributions and of cascade transitions at measured energies (in percent).

Source of uncertainty	Uncertainty (%)			
	1002 keV	1308 keV	1416 keV	1510 keV
Systematics of angular distributions, $E1$	22	14	19	12
$E2$	61	32	47	30
Counting statistics $E1$, $E2$	40	20	10	12
Counting statistics of cascades	50	30	20	20

In general, it is surprising that, in spite of the eminent astrophysical importance of the $^{12}C(\alpha,\gamma)^{16}O$ reaction, the actually measured cross sections and the related uncertainties are not specified in any of the available publications. This complicates the direct comparison of experimental results, since the $E2$ component is strongly affected by the angular distributions used, data that are also not always specified. The role of cascade transitions is also neglected in most cases, which is another soft point in this context.

In conclusion, the present results confirm the latest measurements with HPGe detectors by the Stuttgart group [11,36], but they are not compatible with the larger S_{E1} values reported by Roters *et al.* [14] and Ouellet *et al.* [26].

The second aspect mentioned above, which referred to the sensitivity of the present technique, was studied at the lowest data point at 1008 keV. The statistical uncertainties dominate the total uncertainty in this region, mainly because of the decreasing signal-to-background ratio and not because of the lack of $^{12}C(\alpha,\gamma)$ events. This is an important feature, which bears promising possibilities for further improvements.

Compared to the present situation there are essentially four options: (i) Reduction of beam-induced background because of carbon buildup on the target calls for better and cleaner vacuum, which could be obtained by the use of metal seals, higher pumping capacity, and more efficient cold traps. (ii) Increase of the current on target by means of an optimized beam transport would enhance the capture rate and lower the beam-induced background at the same time. (iii) The resolution in γ-ray energy could be improved by operating the 4π BaF_2 array at lower temperature [40], thus allowing for sharper cuts on the data. (iv) The background from cosmic rays could be further reduced by extending the active shielding to reach complete coverage of the setup.

According to the experience with the present measurement, the combination of these options would lead to a background reduction by a factor of 4. Consequently, the accessible energy range could be pushed to a center-of-mass energy of 750 keV before the present signal-to-background ratio is reached again.

VIII. SUMMARY AND OUTLOOK

The $^{12}C(\alpha,\gamma)^{16}O$ reaction has been measured between $E_{c.m.} = 1002$ and 1510 keV by means of a novel technique using the Karlsruhe 4π BaF_2 detector instead of HPGe detectors. This approach has the advantage of excellent sensitivity because of the high γ efficiency of this array, in particular since the limited energy resolution could be compensated by using a fast pulsed α beam for background suppression. Angular distributions were obtained with good statistics even at the lowest energy due to the 42-fold segmentation of the detector. Measurement and data analysis were accompanied by detailed GEANT simulations to ensure low systematic uncertainties of better than 10%. In this way the $E1$ and $E2$ components could be reliably separated. In addition, the contribution from cascade transitions could be determined for the first time at energies down to 1 MeV.

This work provides useful input to a careful reanalysis of the rate at stellar energies.

Further improvements of the present approach have been considered and have the potential to extend the accessible

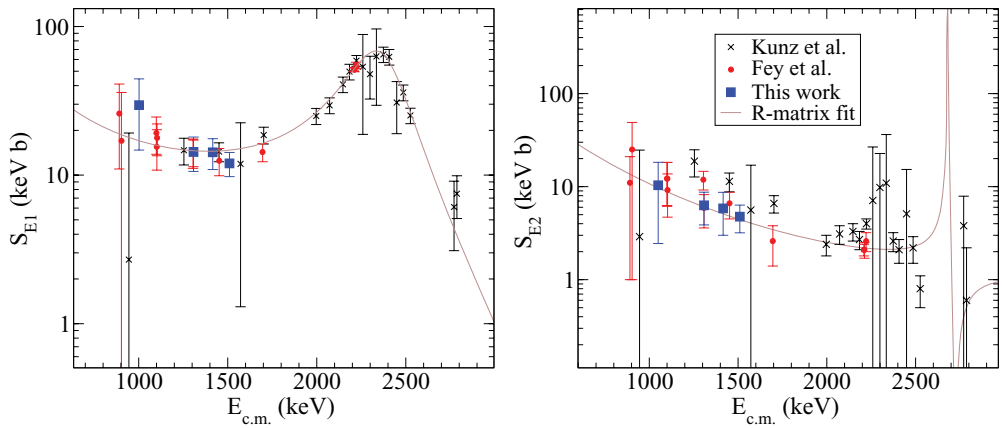

FIG. 8. (Color online) Measured values for the S factor compared with other recent measurements [11,36].

energy range down to center-of-mass energies of 750 keV.

ACKNOWLEDGMENTS

We are grateful to D. Roller, E.-P. Knaetsch, and W. Seith for their continuous support during the measurements and to G. Rupp for his excellent technical assistance. We are also indebted to the SIDONIE group at CSNSM (Orsay, France) for the preparation of the enriched ^{12}C samples and to L. Buchmann (TRIUMF, Vancouver) for providing us with his *R*-matrix code for verifying our own version. This work was supported by the HGF Young Investigators Project No. VH-NG-327 and the EuroGenesis project MASCHE.

[1] E. Burbidge, G. Burbidge, W. Fowler, and F. Hoyle, Rev. Mod. Phys. **29**, 547 (1957).
[2] W. Arnett, Annu. Rev. Astron. Astrophys. **11**, 73 (1973).
[3] C. Angulo *et al*., Nucl. Phys. A **656**, 3 (1999).
[4] T. Rauscher, A. Heger, R. Hoffman, and S. Woosley, Astrophys. J. **576**, 323 (2002).
[5] A. Chieffi and M. Limongi, Astrophys. J. **608**, 405 (2004).
[6] S. E. Woosley, A. Heger, T. Rauscher, and R. Hoffman, Nucl. Phys. A **718**, 3c (2003).
[7] G. Brown *et al*., New Astron **6**, 457 (2001).
[8] C. Abia *et al*., Astrophys. J. **579**, 817 (2002).
[9] M. Lugaro *et al*., Astrophys. J. **593**, 486 (2003).
[10] G. R. Caughlan and W. A. Fowler, At. Data Nucl. Data Tables **40**, 283 (1988).
[11] R. Kunz, M. Jaeger, A. Mayer, J. W. Hammer, G. Staudt, S. Harissopulos, and T. Paradellis, Phys. Rev. Lett. **86**, 3244 (2001).
[12] J. Hammer *et al*., Nucl. Phys. A **758**, 363c (2005).
[13] M. Assunção *et al*., Phys. Rev. C **73**, 055801 (2006).
[14] G. Roters, C. Rolfs, F. Strieder, and H. Trautvetter, Eur. Phys. J. A **6**, 451 (1999).
[15] R. Azuma *et al*., Phys. Rev. C **50**, 1194 (1994).
[16] R. Azuma *et al*., Phys. Rev. C **56**, 1655 (1997).
[17] C. R. Brune, W. H. Geist, R. W. Kavanagh, and K. D. Veal, Phys. Rev. Lett. **83**, 4025 (1999).
[18] C. Brune *et al*., Nucl. Phys. A **688**, 263c (2001).
[19] D. Schürmann *et al*., Eur. Phys. J. A **26**, 301 (2005).
[20] D. Schürmann, A. di Leva, L. Gialanella, D. Rogalla, F. Strieder, N. de Cesare, A. D'Onofrio, G. Imbriani, R. Kunz, C. Lubritto, A. Ordine, V. Roca, C. Rolfs, M. Romano, F. Schümann,, F. Terrasi, H.-P. Trautvetter, The European Physical Journal A **26**, 301 (2006).
[21] C. Matei *et al*., Proceedings of Science PoS **(NIC-IX) 119**.
[22] R. Jaszczak, J. Gibbons, and R. Macklin, Phys. Rev. C **2**, 63 (1970).
[23] R. Jaszczak and R. Macklin, Phys. Rev. C **2**, 2452 (1970).
[24] P. Dyer and C. Barnes, Nucl. Phys. A **233**, 495 (1974).
[25] A. Redder *et al*., Nucl. Phys. A **462**, 385 (1987).
[26] J. Ouellet *et al*., Phys. Rev. C **54**, 1982 (1996).
[27] K. Kettner *et al*., Z. Phys. A **308**, 73 (1982).
[28] L. Gialanella *et al*., Eur. Phys. J. A **11**, 357 (2001).
[29] R. M. Kremer, C. A. Barnes, K. H. Chang, H. C. Evans, B. W. Filippone, K. H. Hahn, and L. W. Mitchell, Phys. Rev. Lett. **60**, 1475 (1988).
[30] H. Trautvetter *et al*., Nucl. Phys. A **621**, 161c (1997).
[31] D. Rogalla *et al*., Nucl. Phys. A **688**, 549c (2001).
[32] N. Ikeda *et al*., Nucl. Phys. A **718**, 558c (2003).
[33] K. Sagara *et al*., Nucl. Phys. A **758**, 427c (2005).
[34] P. Tischhauser *et al*., Phys. Rev. Lett. **88**, 072501 (2002).
[35] K. Wisshak *et al*., Nucl. Instrum. Methods A **292**, 595 (1990).
[36] J. W. Hammer, M. Fey, R. Kunz, J. Kiener, V. Tatischeff, F. Haas, J. L. Weil, M. Assunção, C. Beck, C. Boukari-Pelissie, A. Coc, J. J. Correia, S. Courtin, F. Fleurot, E. Galanopoulos, C. Grama, F. Hammache, S. Harissopulos, A. Korichi, E. Krmpotić *et al*., Nuclear Physics A **752**, 514 (2005).
[37] Application software group, GEANT, Detector description and simulation tool, Computing and Networks Division, CERN, Geneva, Switzerland.
[38] M. Heil *et al*., Nucl. Instrum. Methods A **459**, 229 (2001).
[39] R. Plag, Ph.D. thesis, University of Karlsruhe, Karlsruhe, Germany, 2004 (in German).
[40] K. Wisshak, K. Guber, and F. Käppeler, Nucl. Instrum. Methods A **259**, 583 (1987).